

# Sensing Characterization of Metal Oxide Semiconductor-Based Sensor Arrays for Gas Mixtures in Air

Jung-Sik Kim<sup>†</sup>

Department of Materials Science and Engineering, University of Seoul, Seoul 02504, Republic of Korea

(Received April 4, 2023 : Revised May 17, 2023 : Accepted May 22, 2023)

**Abstract** Micro-electronic gas sensor devices were developed for the detection of carbon monoxide (CO), nitrogen oxides (NO<sub>x</sub>), ammonia (NH<sub>3</sub>), and formaldehyde (HCHO), as well as binary mixed-gas systems. Four gas sensing materials for different target gases, Pd-SnO<sub>2</sub> for CO, In<sub>2</sub>O<sub>3</sub> for NO<sub>x</sub>, Ru-WO<sub>3</sub> for NH<sub>3</sub>, and SnO<sub>2</sub>-ZnO for HCHO, were synthesized using a sol-gel method, and sensor devices were then fabricated using a micro sensor platform. The gas sensing behavior and sensor response to the gas mixture were examined for six mixed gas systems using the experimental data in MEMS gas sensor arrays in sole gases and their mixtures. The gas sensing behavior with the mixed gas system suggests that specific adsorption and selective activation of the adsorption sites might occur in gas mixtures, and allow selectivity for the adsorption of a particular gas. The careful pattern recognition of sensing data obtained by the sensor array made it possible to distinguish a gas species from a gas mixture and to measure its concentration.

**Key words** gas sensor, electronic materials, sol-gel coating, sensing properties.

## 1. Introduction

The metal oxide semiconductor (MOS) sensors have been very popular and widely used for the detection of various oxidizing and reducing gases owing to low cost, simplicity of use, large number of detectable gases and potential gas sensing applications.<sup>1)</sup> On the other hand, MOS gas sensors have serious shortcomings, which are related mainly to their low selectivity, response drifts and wide range of environmental conditions.<sup>2)</sup> MOS gas sensors have four major issues of concern: long-term stability, reproducibility of the devices, selectivity, and sensitivity.<sup>3,4)</sup>

Regarding the selectivity issue, the concept of an e-nose has been developed to achieve the ability of classifying complex gas mixtures, such as aromas and odors, using cross-sensitive sensors.<sup>5-7)</sup> The characteristics of individual sensors belonging to the sensor array should be as diverse as possible to ensure that the partial sensor gas responses are non-correlated and can enable the instrument to discriminate gases and

gas mixtures reliably. As another issue, the extensive dissemination of such e-noses in various areas requires high reproducibility of the sensor arrays, high training cost and a shortage of MOS gas sensors with long-term stability. This appears to be one of the key challenges that require a breakthrough.<sup>8)</sup> Gas sensor microarrays based on a single metal oxide thin film segmented by electrodes appear to meet this requirement because a large number of chips have been produced using the same fabrication process, and sensor segments are expected to be similar. On the other hand, such multi-sensor microarrays still depend on non-controlled variations during the manufacturing process. In particular, the sputtering of current-injecting micro-electrodes for the conductivity measurements results frequently in the substantial and non-predictable doping of sensing areas with an electrode material, which alters the resistance of the sensing segments in a random manner. Minimizing the influence of these uncontrollable contaminations would provide a good

<sup>†</sup>Corresponding author

E-Mail : jskim@uos.ac.kr (J.-S. Kim, Univ. Seoul)

© Materials Research Society of Korea, All rights reserved.

This is an Open-Access article distributed under the terms of the Creative Commons Attribution Non-Commercial License (<http://creativecommons.org/licenses/by-nc/3.0>) which permits unrestricted non-commercial use, distribution, and reproduction in any medium, provided the original work is properly cited.

step towards reproducible multi-sensor arrays. Finally, the reported sensitivity of many MOS gas sensors is surprisingly high.<sup>9-11)</sup> The current detection limits for many reducing gases are sufficient for major practical applications, making the sensitivity issue a lesser concern. On the other hand, the higher gas-sensitivity observed by nano-crystal based metal oxide layers tends to decrease during the course of exploitation,<sup>12)</sup> whereas relatively stable sensing structures, such as meso/nano-wires or stabilized crystallite films, often have comparably lower sensitivities.<sup>13,14)</sup> Therefore, improving the stability of the sensing properties of MOS sensors is a major issue.

Gas identification has attracted considerable attention over the past twenty years. The ability to monitor and measure the leakage of combustible and explosive gases precisely is essential for preventing accidental explosions or other issues, such as toxicity. Accordingly, there is urgent demand for sensors combined with pattern recognition systems that can detect and determine the various kinds of combustible gases selectively.<sup>15,16)</sup>

Carbon monoxide (CO) and ammonia (NH<sub>3</sub>) are reducing gases, while nitrogen oxides (NO<sub>x</sub>) and formaldehyde (HCHO) are oxidizing gases. Giri et al.<sup>17)</sup> investigate on the gas sensing properties of both oxidising and reducing gases by nanoscale Co<sub>3</sub>O<sub>4</sub> powders and demonstrated its sensing mechanism.

In this study, micro electro mechanical systems (MEMS)-based MOS gas sensors, which have a number of interesting features and are particularly attractive for their practical interest, were used. Previous studies developed four gas sensors based on MEMS platforms for the detection different gases, carbon monoxide (CO), nitrogen oxides (NO<sub>x</sub>), ammonia (NH<sub>3</sub>), and formaldehyde (HCHO). Four sensing materials with nano-sized particles for these target gases (Pd-SnO<sub>2</sub> nano-powder for CO, In<sub>2</sub>O<sub>3</sub> nano-particle for NO<sub>2</sub>, Ru-WO<sub>3</sub> nano-composite for NH<sub>3</sub>, and hybridized SnO<sub>2</sub>-ZnO material for HCHO) were synthesized using a sol-gel method.<sup>18,19)</sup> Each MEMS gas sensor exhibited good sensing performance for their target gases, and the optimal points for micro-heater operation were examined during temperature modulation in micro-platforms.

In previous studies, systems for evaluating the gas sensing performance were set up to identify the sensing properties in mixed gas systems, particularly binary mixed systems. After

characterizing the gas sensing properties under single gas atmospheric conditions, the gas sensing performance of the three sensors were characterized and examined in a binary mixed system. From the experimental data in the MEMS gas sensor arrays, the sensor characteristics for each sensor device, gas sensing behavior and sensor response in mixed gas systems were examined.

## 2. Experimental

The gas sensing elements for the detection of their target gases, SnO<sub>2</sub> for CO, In<sub>2</sub>O<sub>3</sub> for NO<sub>2</sub>, WO<sub>3</sub> for NH<sub>3</sub>, and SnO<sub>2</sub>-ZnO for HCHO, were synthesized using the sol-gel based method.<sup>18,19)</sup> One drop of each sol with a sensing material was placed on the electrode of the sensor platform, and the sensor chips were then heat-treated at their sintering temperatures. Fig. 1 shows field emission scanning electron microscopy (FESEM) images of the four sensing materials. As shown in (c), WO<sub>3</sub> particles are relatively large to be micrometer-sized, whereas (a) SnO<sub>2</sub>, (b) In<sub>2</sub>O<sub>3</sub> and (d) SnO<sub>2</sub>-ZnO particles are mostly nano-sized. In general, the precipitation of WO<sub>3</sub> · nH<sub>2</sub>O from a tungsten sol using concentrated tungstic acid and hydrogen peroxide occurs rapidly, often yielding micrometer (or larger) sized WO<sub>3</sub> particles.<sup>20)</sup>

Several types of co-planar type micro gas sensor platforms were designed and fabricated previously using the MEMS process.<sup>21)</sup> The sensor chip size of the MEMS platform was 1.8 mm × 1.8 mm, and a Pt thin-film layer was patterned for the sensing electrode and micro-heater. In this study, the sensor device with an S-shaped micro-heater pattern was adapted because of its low power consumption and stable process for the application of sensing materials [Fig. 2(a)]. The fabricated MEMS gas sensors had low power dissipation, and the power consumption increased linearly with increasing operation temperature, as shown in Fig. 2(b). The optimized operating temperatures of the sensor devices were 225 °C for the Pd-SnO<sub>2</sub> and In<sub>2</sub>O<sub>3</sub> sensors, and 360 °C for the Ru-WO<sub>3</sub> and SnO<sub>2</sub>-ZnO sensors, which had a power consumption of 35.26 mW and 64.37 mW, respectively.<sup>18,19)</sup>

The four gas sensors were evaluated in gas mixtures using a continuous gas system, and four sensors were placed in the test chamber. The test chamber was connected to a computer-supervised continuous flow system that produced the desired concentrations of the different gases and gas mixtures in a

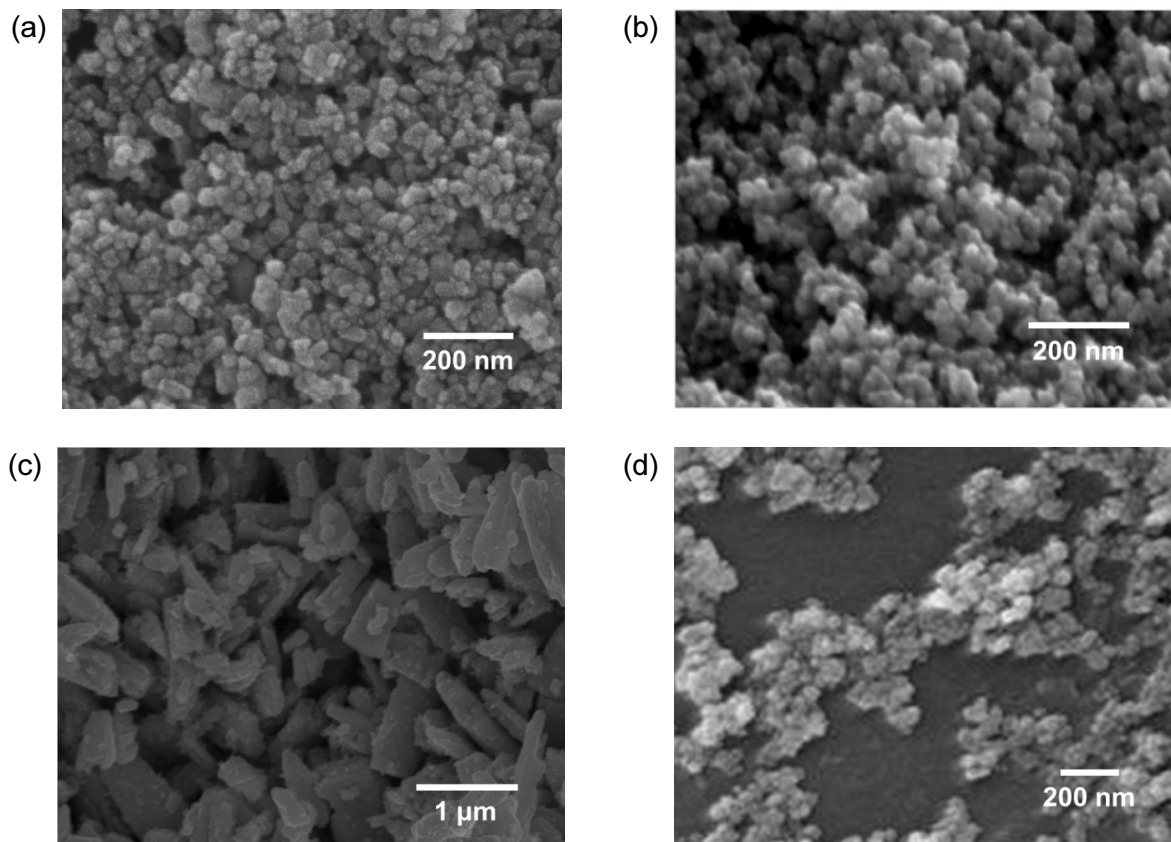


**Fig. 1.** Micro-structures of the four gas sensing materials: (a) Pd-SnO<sub>2</sub>, (b) In<sub>2</sub>O<sub>3</sub>, (c) Ru-WO<sub>3</sub>, and (d) Pd doped SnO<sub>2</sub>-ZnO.

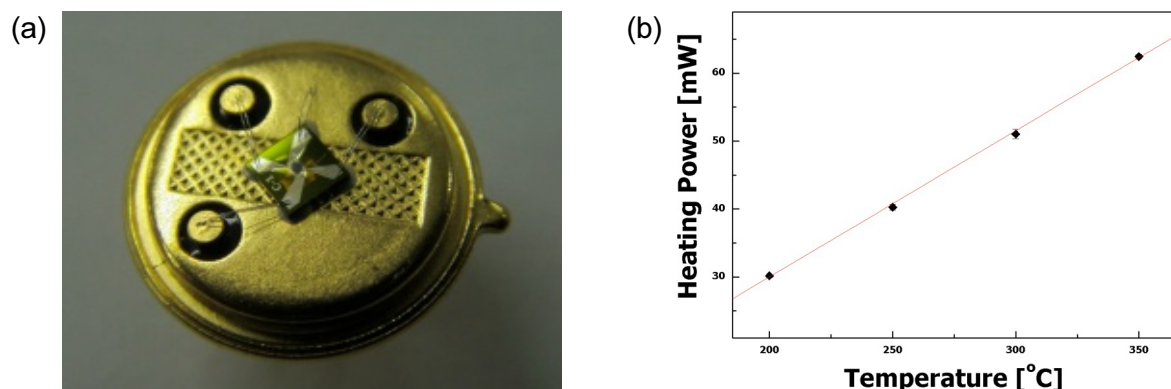


**Fig. 2.** Characteristics of the micro gas sensors: (a) electro-thermal property and (b) sensor photographs with TO-39 package.

highly reproducible manner. The test gases (CO, NO<sub>2</sub>, NH<sub>3</sub>, and HCHO) diluted with nitrogen gas were carried with dry air at a constant flow rate. The total gas flow rate was set to 500 ml/min. The concentration in each test gas was 0~60 ppm for CO, 0~0.6 ppm for NO<sub>2</sub>, 0~10.0 ppm for NH<sub>3</sub>, and 0~5.0 ppm for HCHO. Table 1 lists the six gas mixtures (CO-NO<sub>2</sub>, CO-NH<sub>3</sub>, CO-HCHO, NO<sub>2</sub>-NH<sub>3</sub>, NO<sub>2</sub>-HCHO and NH<sub>3</sub>-HCHO) along with their mixing conditions. Table 2 defines four fabricated gas sensors (SN, IN, WO, and SZ)

with sensing materials.

To quantify the sensor responses for both oxidizing and reducing gases as well as their mixtures, the gas sensitivity (*S*) was defined as follow;

$$S = \log \left( \frac{R_g}{R_a} \right) \quad (1)$$

where *R<sub>a</sub>* is the sensor resistance in air and *R<sub>g</sub>* is the sensor

**Table 1.** Mixed gas systems for the characterization of single gases and their mixtures.

CO (ppm) \ NO <sub>2</sub> (ppm)	0	30	60	CO (ppm) \ NO <sub>2</sub> (ppm)	0	30	60
0		#1	#2	0		#1	#2
0.3	#3	#4	#5	5.0	#3	#4	#5
0.6	#6	#7	#8	10.0	#6	#7	#8
CO (ppm) \ HCHO (ppm)	0	30	60	NO <sub>2</sub> (ppm) \ NH <sub>3</sub> (ppm)	0	0.3	0.6
0		#1	#2	0		#1	#2
2.5	#3	#4	#5	5.0	#3	#4	#5
5.0	#6	#7	#8	10.0	#6	#7	#8
NO <sub>2</sub> (ppm) \ HCHO (ppm)	0	0.3	0.6	NH <sub>3</sub> (ppm) \ HCHO (ppm)	0	5.0	10.0
0		#1	#2	0		#1	#2
2.5	#3	#4	#5	2.5	#3	#4	#5
5.0	#6	#7	#8	5.0	#6	#7	#8

**Table 2.** Main features of each sensing materials.

	Composition	Average particle size	Operating temperature (°C)
SN	1 % Pd-SnO <sub>2</sub>	40 nm	267
IN	In <sub>2</sub> O <sub>3</sub>	70 nm	267
WO	1 % Ru-WO <sub>3</sub>	1.0 μm	334
SZ	1 % Pd + SnO <sub>2</sub> -ZnO	20 nm	367

resistance after injecting the target gas. The gas sensitivity showed negative values ( $S < 0$ ) for reducing gases, and positive values ( $S > 0$ ) for oxidizing gases because all sensors were simultaneously sensitive to both reducing (CO, NH<sub>3</sub> and HCHO) and oxidizing (NO<sub>2</sub>) gases. The gas sensing properties and selective reactions to several gases were analyzed by quantifying the sensitivity.

### 3. Results and Discussion

Before the mixed gas sensing test, two cases of the sensing behaviors were assumed for the sensor responses. One is that the test sensor shows a gas selective response to other gases, and the other is that the sensor has no selectivity for all gases. Initially, gas sensor materials without selectivity might possess multi-functional adsorption sites for both gases during mixed gas flow. In an oxidizing and reducing gas mixture, both gases would adsorb on the surface of the sensing material, and the number of adsorbed gas molecules would be in the same proportion as that of each single gas. If the

oxidation effect on the total sensor conductance prevails, a specific amount of oxidizing gas would counterbalance the reducing gases, and the remaining oxidizing species might contribute to the change (augment) in conductance. Therefore, a change in conductance might occur in the form of a subtraction reducing effect from oxidizing reactions. Otherwise, in the case of a mixture with reducing agents, a change in conductance might manifest as the summation of the same type reactions (reducing effects), which can have a synergic effect on the reaction of each species.

On the other hand, gas sensing materials with good selectivity might have a single type of adsorption site for a specific gas in a mixed gas system. For example, a sensing material sensitive to an oxidizing gas would show a response to an oxidizing gas but not to a reducing gas, even in an oxidizing-reducing gas mixture. In addition, in the same type gas mixture (e.g. reducing gas mixtures), the sensing materials might exhibit a response toward the target gas (adsorbed gas on the sensing element), but ignore the other gases in the experiments.

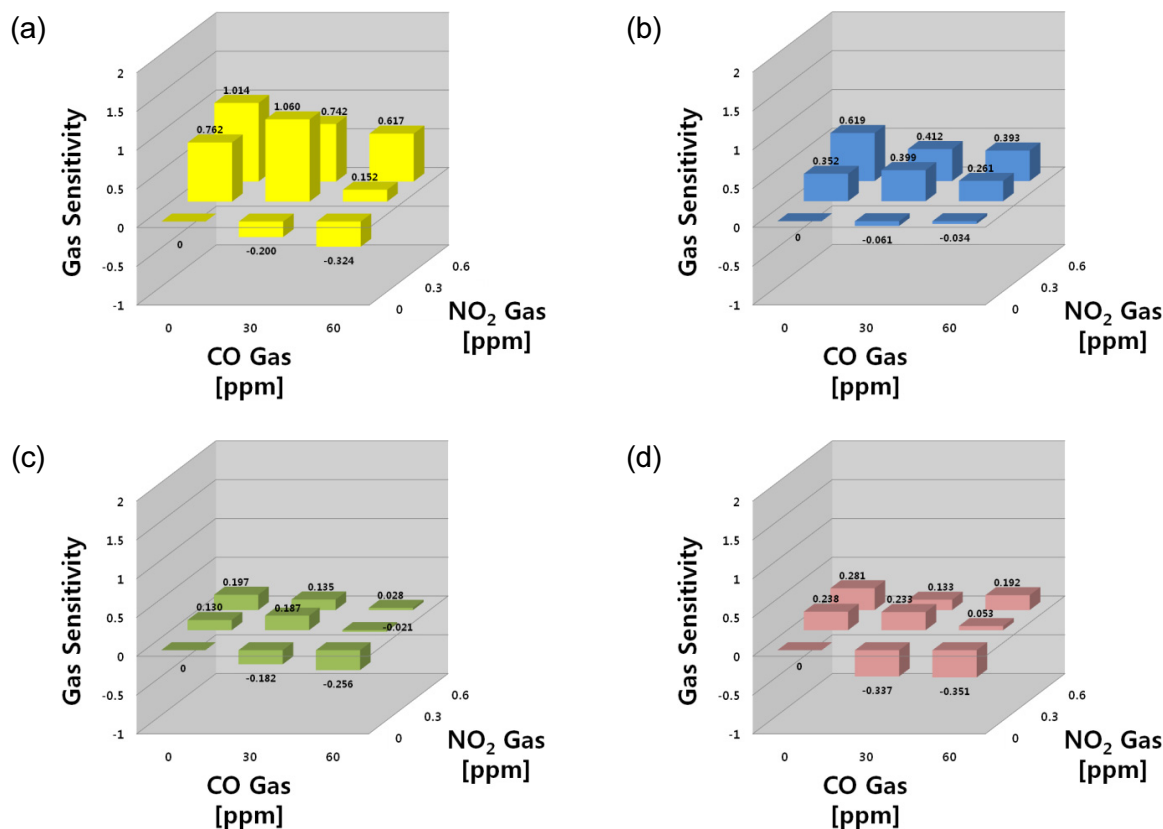


**Fig. 3.** Gas sensing properties in the CO-NO<sub>2</sub> system; (a) SN, (b) IN, (c) WO, and (d) SZ sensors.

For the gas mixture of CO-NO<sub>2</sub> containing both reducing and oxidizing gas, the sensing response to NO<sub>2</sub> gas was higher than that of CO in all four sensors. Fig. 3 shows the variations of the gas sensitivity of all sensors to CO and NO<sub>2</sub> gases and their mixtures. All sensors showed stronger responses to NO<sub>2</sub> gas than CO, and the sensitivity showed positive values in the presence of NO<sub>2</sub> gas. The SN sensor exhibited a strong response to both gases and their mixtures, whereas the IN sensor responded only to NO<sub>2</sub>. The WO and SZ sensors exhibited similar behaviors to the SN sensor, but their sensitivities to NO<sub>2</sub> gas were slightly lower.

In the CO-NH<sub>3</sub> set as shown in Fig. 4, the CO gas responses were much higher than NH<sub>3</sub> gas in a mixture of reducing agents, but the sensitivities in the gas mixture were higher than that to each gas separately under most experimental conditions. The SN and SZ sensors were more sensitive to their target gas (CO) than NH<sub>3</sub> within the test ranges:  $S = -0.179$  and  $-0.420$  for SN, and  $S = -0.100$  and  $-0.176$  for SZ sensors (at CO 30 ppm and 60 ppm). On the other hand, the changes in resistance were slightly lower in the case of a gas mixture. The IN sensor responses were quite poor to both

gases and showed a selective response to both gases. The WO and SZ sensors were sensitive to both the single gases and their mixtures, with higher sensitivities observed with the gas mixtures. For the tests in a mixture of reducing agents, the sensor responses targeting these gases did not show any synergic effects. The sensitivity of the SN sensor was  $-0.420$  for 60 ppm CO gas, but the sensitivity was slightly lower ( $S = -0.327$ ) for CO 60 ppm - NH<sub>3</sub> 2.5 ppm. This phenomenon was not observed in the other sensors, which had gas selectivity for the specific gas species. In three mixtures (CO 60 ppm - NH<sub>3</sub> 0 ppm, CO 60 ppm - NH<sub>3</sub> 5.0 ppm, and CO 60 ppm - NH<sub>3</sub> 10.0 ppm), the CO concentration was identical. As the NH<sub>3</sub> concentration increased, however, the sensitivity of the SN sensor was slightly lower for the gas mixtures than for the single CO gas. This suggests that the specific adsorption and selective activation of adsorption sites might occur in gas mixtures and offer a priority for the adsorption of a specific gas, which will be discussed in the following section.

Fig. 5 shows gas sensing properties for the target gas of CO-HCHO mixture. The gas responses of SN, WO and SZ sensors in the CO-HCHO system showed similar behavior in

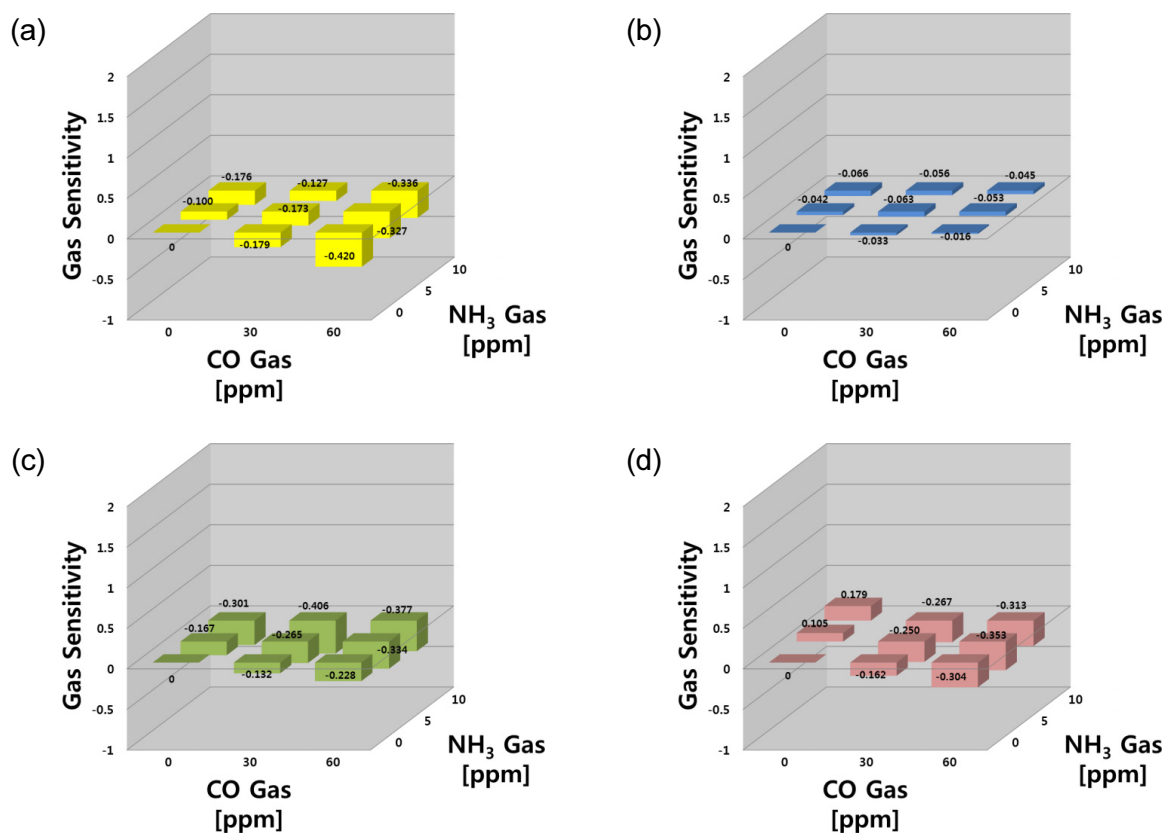


**Fig. 4.** Gas sensing properties in the CO-NH<sub>3</sub> system; (a) SN, (b) IN, (c) WO, and (d) SZ sensors.

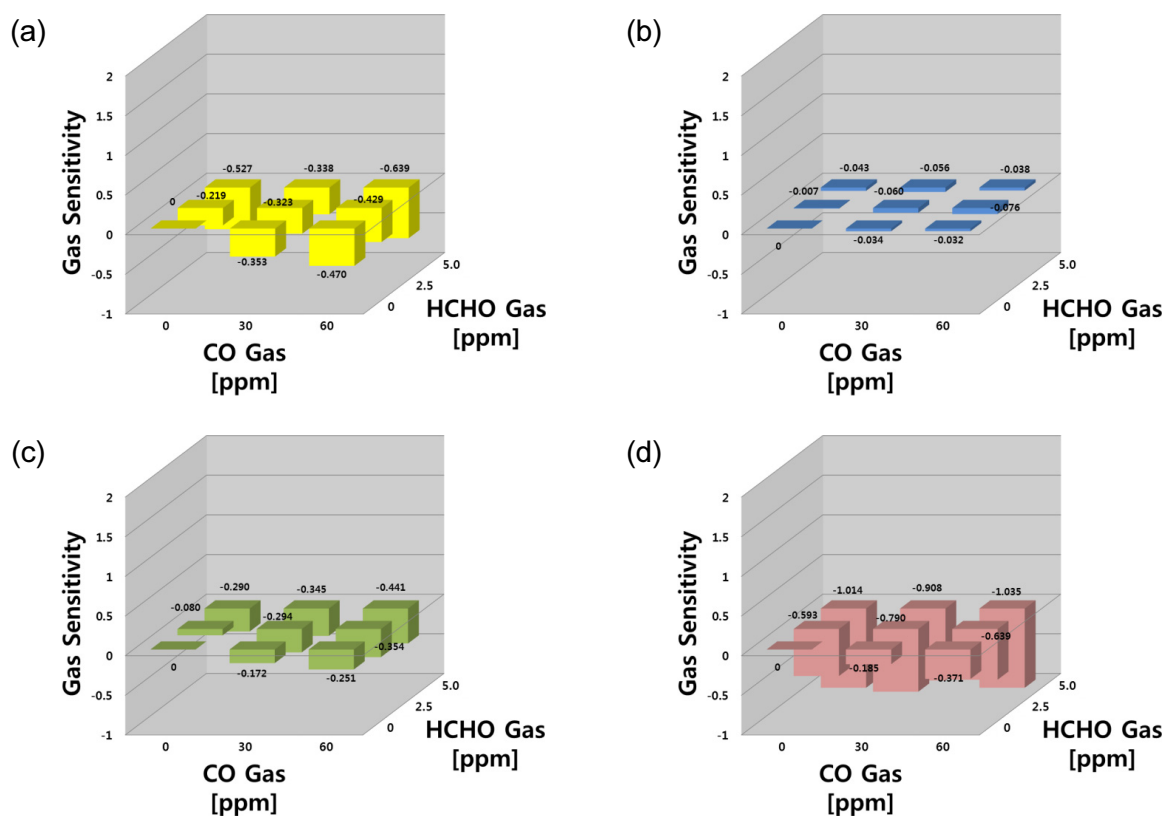


**Fig. 5.** Gas sensing properties in the CO-HCHO system; (a) SN, (b) IN, (c) WO, and (d) SZ sensors.

the CO-NH<sub>3</sub> system, whereas the IN sensor showed no responses for both gases. Three sensors (SN, WO and SZ) were sensitive to both the single gases and their mixtures, with higher sensitivities observed with the gas mixtures. Moreover, the SZ sensor responses toward HCHO were stronger than CO gas. Similar to the CO-NH<sub>3</sub> system, there was no synergic effect in the SN sensor responses to a mixture of CO and HCHO. The sensitivity of the SN sensor was -0.470 for 60 ppm CO gas, but the sensitivity was slightly lower ( $S = -0.429$ ) for CO 60 ppm - HCHO 2.5 ppm. This also suggests that the specific adsorption and selective activation offer priority for the adsorption of a specific gas in the gas mixtures.

Fig. 6 shows gas sensing properties for the target gas of NO<sub>2</sub>-NH<sub>3</sub> mixture. In the NO<sub>2</sub>-NH<sub>3</sub> system, the responses to NO<sub>2</sub> gas were stronger than those of NH<sub>3</sub>. In the SN sensor, the sensitivities exhibited increasing behavior to NO<sub>2</sub> and decreasing behavior to NH<sub>3</sub> at higher concentrations, showing that the sensor responds to both gases ( $S = 0.934$  at 0.3 ppm). In the gas mixtures, the changes in resistance were higher than the baseline ( $R_a$ ) and decreased with increasing NH<sub>3</sub> concentration. On the other hand, the sensitivities to both

gases had positive values ( $S > 0$ ) within the test ranges. The IN sensor had a selective response to NO<sub>2</sub> gas but was barely sensitive to NH<sub>3</sub> gas. As the NH<sub>3</sub> gas concentration increased, the IN sensor exhibited a slight decrease in sensitivity to NO<sub>2</sub> gas in the NO<sub>2</sub>-NH<sub>3</sub> mixed gas system. The WO sensor showed similar behavior to the IN sensor, as well as a very selective response to both gases, but it was more sensitive to NO<sub>2</sub> gas.

For the NO<sub>2</sub>-HCHO mixture as shown in Fig. 7, the responses to NO<sub>2</sub> gas were stronger than those of HCHO. In the SN and WO sensors, the sensitivities showed increasing behavior to NO<sub>2</sub> and decreasing behavior to HCHO at higher concentrations. On the other hand, the IN sensor showed a selective response to NO<sub>2</sub> gas, but little sensitivity to HCHO gas. As the HCHO gas concentration increased, the IN sensor showed a slight decrease in sensitivity to NO<sub>2</sub> gas in the NO<sub>2</sub>-HCHO mixed gas system. The WO sensor showed similar behavior to the IN sensor, as well as a very selective response to both gases, but it was more sensitive to NO<sub>2</sub> gas. The SZ sensor responses toward HCHO were stronger than NO<sub>2</sub> gas for the NO<sub>2</sub> and HCHO gas mixture.

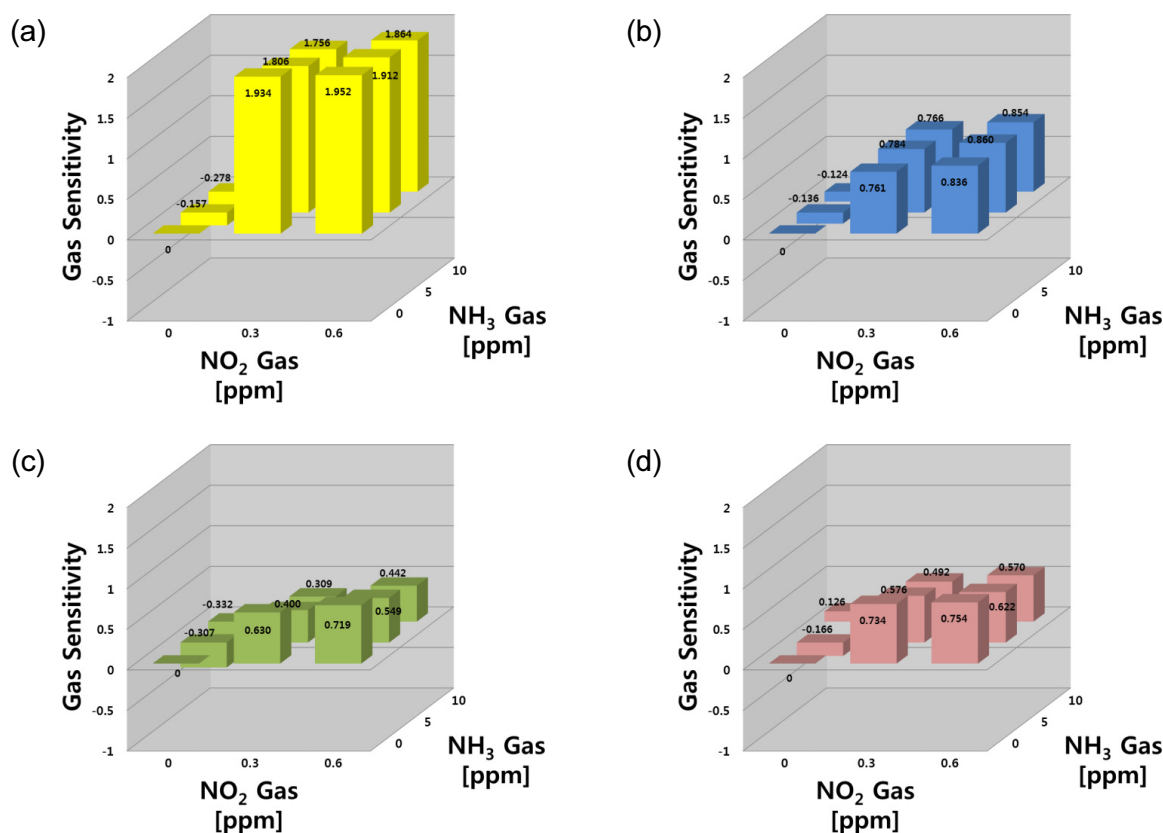


Fig. 6. Gas sensing properties in the NO<sub>2</sub>-NH<sub>3</sub> system; (a) SN, (b) IN, (c) WO, and (d) SZ sensors.



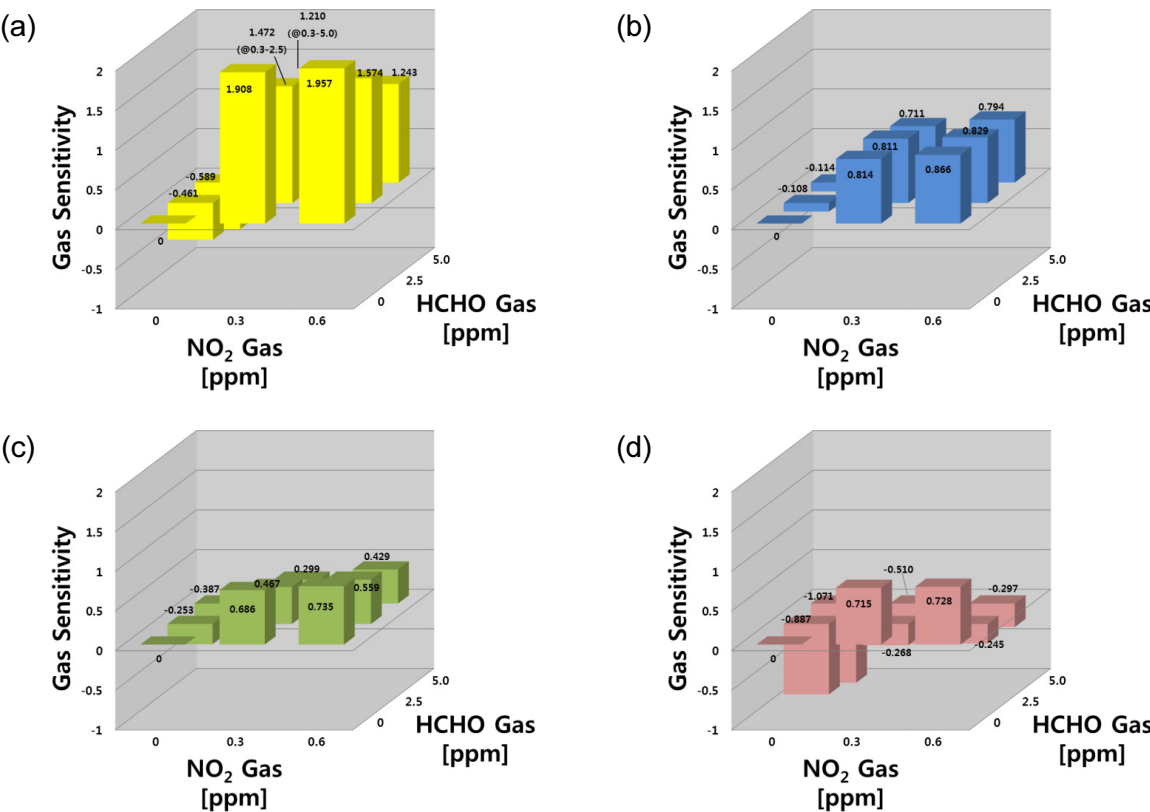


Fig. 7. Gas sensing properties in the NO<sub>2</sub>-HCHO system; (a) SN, (b) IN, (c) WO, and (d) SZ sensors.

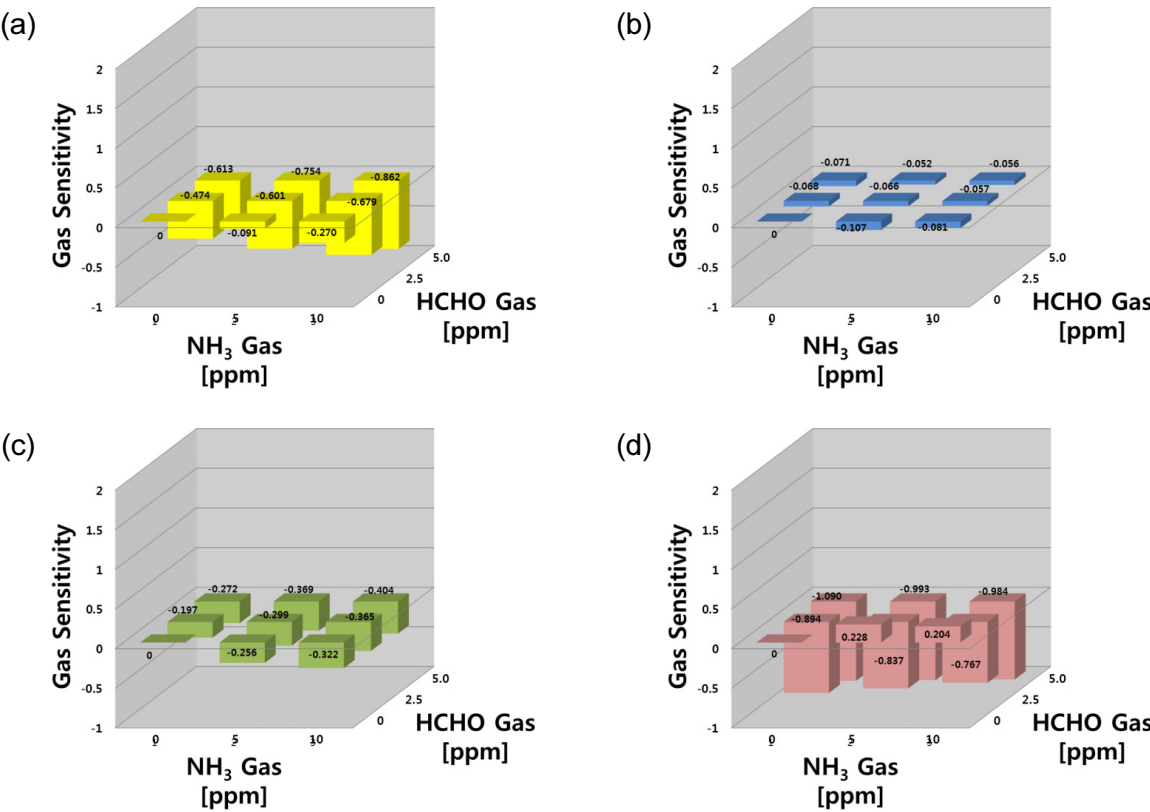


Fig. 8. Gas sensing properties in the NH<sub>3</sub>-HCHO system; (a) SN, (b) IN, (c) WO, and (d) SZ sensors.



Fig. 8 shows gas sensing properties for the target gas of  $\text{NH}_3$ -HCHO mixture. For the final set of  $\text{NH}_3$ -HCHO system, the gas responses of the SN, WO and SZ sensors showed similar behavior in both reducing agent systems ( $\text{CO}$ - $\text{NH}_3$ , and  $\text{CO}$ -HCHO systems), whereas the IN sensor showed no responses to both gases. Three sensors (SN, WO and SZ) were sensitive to both the single gases and their mixtures, with higher sensitivities observed with the gas mixtures, and the SZ sensor responses toward HCHO were stronger than to  $\text{NH}_3$  gas. In this system, consistent with the two reducing agents, there was no synergic effect in the SN sensor responses to a mixture of  $\text{NH}_3$  and HCHO.

Overall, the IN sensor could detect  $\text{NO}_2$  selectively, whereas the SN sensors detected all four ( $\text{CO}$ ,  $\text{NO}_2$ ,  $\text{NH}_3$ , HCHO) gases. If coupled with an IN sensor, SN is capable of detecting  $\text{NO}_2$  sensitively. On the other hand, the gas sensitivity signals of the two sensors were not sufficient for the detection of all four gases. The WO and SZ sensors detected all four gases but had low gas selectivity. Therefore, the four-sensor-array would be sufficient to discriminate mixtures of these gases. To gain clear insight into the applicability of the sensor array in this application, the responses with sensitivity can be arranged in a  $4 \times 4$  matrix, in which each element represents the response of each sensor to each target gas. This matrix suggests how the different gas contributions can be extrapolated from the sensor array data using the signal process.

Recently, many research groups have examined the sensor response to various harmful gases and their mixtures, and reported the gas sensing patterns.<sup>22,23)</sup> In particular, they characterized multi-sensor responses, analyzed the feature abstraction of the raw signals, and recognized the data patterns for the accurate monitoring of harmful gases. The present study analyzed the sensing properties of micro gas sensor arrays by examining the raw data in the gas mixtures.

## 4. Conclusion

Four gas sensors based on MEMS platforms were developed for the detection of  $\text{CO}$ ,  $\text{NO}_x$ ,  $\text{NH}_3$ , and HCHO gases. Three sensing materials with nano-sized particles ( $\text{Pd-SnO}_2$  for  $\text{CO}$ ,  $\text{In}_2\text{O}_3$  for  $\text{NO}_2$ ,  $\text{Ru-WO}_3$  for  $\text{NH}_3$ , and  $\text{SnO}_2$ - $\text{ZnO}$  for HCHO) were synthesized using a sol-gel method. Each MEMS gas sensor exhibited good sensitivity to their target

gases, and the optimal number of points for micro-heater operation was examined. The sensor characteristics for each sensor device and the gas sensing behaviors in the mixed gas system were analyzed using the experimental data in the MEMS gas sensor arrays. The gas sensing behaviors to the mixed gas systems suggest that specific adsorption and selective activation of adsorption sites might occur in gas mixtures and offer priority for the adsorption of a specific gas. An analysis of the sensing performance of the sensor arrays will make it possible to discriminate the components in harmful gas mixtures as well as their concentrations using pattern recognition techniques.

## Acknowledgement

This study was supported by the 2022 Research Fund of the University of Seoul.

## References

1. D. Degler, U. Weimar and N. Barsan, *ACS Sens.*, **4**, 2228 (2019).
2. Y. K. Gautam, K. Sharma, S. Tyagi, A. K. Ambedkar, M. Chaudhary and B. P. Singh, *R. Soc. Open Sci.*, **8**, 2013244 (2021).
3. A. Vergara, E. Llobet, J. Brezmes, P. Ivanov, C. Cane, I. Gracia, X. Vilanova and X. Correig, *Sens. Actuators, B*, **123**, 1002 (2007).
4. I. Kiselev, M. Sommer, J. K. Mann and V. V. Sysoev, *IEEE Sens. J.*, **10**, 849 (2010).
5. K. Persaud and G. Dodd, *Nature*, **299**, 352 (1982).
6. U. Weimar and W. Gopel, *Sens. Actuators, B*, **52**, 143 (1998).
7. J. Zhang, Z. Qin, D. Zeng and C. Xie, *Phys. Chem. Chem. Phys.*, **19**, 6313 (2017).
8. B. Sharma, A. Sharma and J.-S. Kim, *Sens. Actuators, B*, **262**, 758 (2018).
9. P. Althainz, J. Goschnick, S. Ehrmann and H. J. Ache, *Sens. Actuators, B*, **33**, 72 (1996).
10. P. Ivanov, E. Llobet, X. Vilanova, J. Brezmes, J. Hubalek and X. Correig, *Sens. Actuators, B*, **99**, 201 (2004).
11. K. Sun, G. Zhan, L. Zhang, Z. Wang and S. Lin, *Sens. Actuators, B*, **379**, 133294 (2023).
12. V. V. Sysoev, T. Schneider, J. Goschnick, I. Kiselev, E. Strelcov and A. Kolmakov, *Sens. Actuators, B*, **139**, 699 (2009).
13. V. V. Sysoev, K. B. Button, K. Wepsiec, S. Dmitriev and A. Kolmakov, *Nano Lett.*, **6**, 1584 (2006).

14. H. Huang, Y. C. Lee, C. L. Chow, O. K. Tan, M. S. Tse and T. White, *Sens. Actuators, B*, **138**, 201 (2009).
15. S. Minghua, *IEEE Trans. Instrum. Meas.*, **55**, 1786 (2006).
16. S. Zhang, C. Xie, D. Zeng, H. Li, Z. Bai and S. Cai, *IEEE Sens. J.*, **8**, 1816 (2008).
17. S. Giri, P. N. Anantharamaiah and B. Sahoo, *Adv. Powder Technol.*, **33**, 103529 (2022).
18. S. D. Kim, B. J. Kim, J. H. Yoon and J. S. Kim, *J. Korean Phys. Soc.*, **51**, 2069 (2007).
19. J.-H. Yoon and J.-S. Kim, *Adv. Mater. Res.*, **74**, 255 (2009).
20. M. Breedon, P. Spizzirri, M. Taylor, J. d. Plessis, D. McCulloch, J. Zhu, L. Yu, Z. Hu, C. Rix, W. Wlodarski and K. Kalantar-zadeh, *Cryst. Growth Des.*, **10**, 430 (2010).
21. W. S. Choi, B. J. Kim, H. J. Lee, J. W. Choi, S. D. Kim and N. K. Min, *J. Nanosci. Nanotechnol.*, **12**, 1 (2012).
22. K. Minami, G. Imamura, T. Nemoto, K. Shiba and G. Yoshikawa, *Mater. Horiz.*, **6**, 580 (2019).
23. H. Ji, Y. Liu, R. Jhang, Z. Yuan and F. Meng, *Sens. Actuators, B*, **376**, 132969 (2023).

## Author Information

### Jung-Sik Kim

Professor, Department of Materials Science and Engineering,  
University of Seoul